Supplementary file

Three-terraced evaporated ramp model for differentiation of the massive dolomitization process: Insights from the Lower Cambrian Longwangmiao Formation in the Sichuan Basin

Xin Jin[1], Jinmin Song[1*], Shugen Liu[1], Zhiwu Li[1], Di Yang[1], Han Wang[1,2]

[1] *State Key Laboratory of Oil and Gas Reservoir Geology and Exploitation, Chengdu University of Technology, Chengdu 610059, P. R. China*

[2] *Department of Earth Sciences, University of Leeds, Leeds LS2 9JT, UK*

E-mail address: xinjin96@outlook.com (X. Jin); songjinmin2012@cdut.edu.cn (J. Song); lsg@cdut.edu.cn (S. Liu); lizhiwu06@cdut.edu.cn (Z. Li); yangdi6202205@126.com (D. Yang); wanghan@cdut.edu.cn (H. Wang).

* Corresponding author (ORCID: 0000-0003-3225-3750)

Jin, X., Song, J., Liu, S., Li, Z., Yang, D., Wang, H. Three-terraced evaporated ramp model for differentiation of the massive dolomitization process: Insights from the Lower Cambrian Longwangmiao Formation in the Sichuan Basin. Advances in Geo-Energy Research, 2025, 15(3): 216-229.

The link to this file is: https://doi.org/10.46690/ager.2025.03.05

Supplementary Text

METHODS

Quantitative powder X-ray diffractometry was performed using a Bruker D2 Phaser instrument at the Geochemistry Laboratory at Chengdu University of Technology.

Analysis of the carbon and oxygen isotopes was performed using a Finnigan MAT253 gas mass spectrometer using the McCrea orthophosphate-dissolution technique and the NBS-18 standard in the Geochemistry Laboratory at Chengdu University of Technology. *In-situ* laser carbon and oxygen isotope analysis was completed at PetroChina Hangzhou Research Institute of Geology using a Finnigan MAT253 mass spectrometer.

The major and trace elements analysis was completed at the Research Institute of Qinghai–Tibetan Plateau, Chinese Academy of Sciences. The major element analysis was conducted using an Inductively Coupled Plasma Optical Emission Spectrometer (ICP-OES) (PerkinElmer Company, model 5300V). Trace element analysis was conducted using an Inductively Coupled Plasma Mass Spectrometer ELAN DRC-e ICP-MS (PerkinElmer, USA). The concentrations of rare earth elements (REEs) are normalized using the Seawater standard (Kawabe et al., 1998). Eu anomalies (Eu/Eu*) and Ce anomalies(Ce/Ce*) are calculated as follow: $\delta Eu=2\times Eu_n/(Sm_n+Gd_n)$ (Bau and Dulski, 1996); $\delta Ce=Ce_n/(2\times Pr_n-Nd_n)$ (McLennan, 1989);. $(La/Yb)_n=La_n/Yb_n$; ΣREE = SUM(La, Ce, Pr, Nd, Sm, Eu, Gd, Tb, Dy, Ho, Er, Tm, Yb, Lu); ΣLREE = SUM(La, Ce, Pr, Nd, Sm, Eu); ΣHREE = SUM(Gd, Tb, Dy, Ho, Er, Tm, Yb, Lu); the value marked by the symbol $_n$ is standardized by seawater; $REE_n = REE/(REEs \times 10^6)$.

Strontium isotope analysis was conducted using a Finnigan MAT-262 multi-collector thermal ionisation mass spectrometer at the State Key Laboratory of Reservoir Geology and Exploitation, Chengdu University of Technology.

Cathodoluminescence (CL) analysis was conducted at Southwest Petroleum University using a CL8200MK5 cold cathode device mounted on a CL microscope.

In-situ trace element analysis was completed by Wuhan Sample Solution Analytical Technology Co., Ltd., China. The *in-situ* analysis of the trace elements in minerals were determined using the LA-ICP-MS electron probe method. The GeolasPro laser ablation system was composed of a COMPexPro 102 ArF 193 nm excimer laser and a MicroLas optical system, with the ICP-MS model being Agilent 7900.

In-situ Sr isotope ratios were measured by a Neptune Plus MC-ICP-MS in combination with a Geolas HD excimer ArF laser ablation system at the Wuhan SampleSolution Analytical Technology Co., Ltd, Hubei, China.

Calcium isotope analysis was conducted using a Finnigan MAT-262 multi-collector thermal ionisation mass spectrometer at the State Key Laboratory of Reservoir Geology and Exploitation, Chengdu University of Technology.

The synthetic seismogram manufactures have been accomplished by using 35 Hz rake wavelet. One 2D seismic lines with a length of approximately 800 km were interpreted through boreholes for comparison of wave groups and energy characteristics.

SUPPLEMENTAL ASSESSMENT OF DIAGENETIC EFFECTS

(1) Evaluation of diagenetic alterations

The Mn/Sr ratios can be divided into three groups as < 2, 2 to 10, and > 10 to characterize little, mild and strong alteration extents. In the lower terrace, the Mn/Sr ratios are 0.24 to 3.58 ($n = 41$) which points to little diagenetic alteration. In the medium terrace, the Mn/Sr ratios are 0.97 to 5.64 ($n = 31$), indicating a mild extent of diagenetic alteration. The Mn/Sr ratios range from 4.34 to 9.98 ($n = 46$) in the higher terrace, implying mild diagenetic alteration to be effective indicators of the early diagenetic phase.

Within the Sichuan Basin, the average $\delta^{18}O$ values are −6.82 ‰, −7.49 ‰, and −7.79 ‰, respectively, in the higher, lower and medium terrace, all suggesting little diagenetic alteration.

(2) Evaluation of detrital influence

The whole rock samples of the dolostone exhibit relatively high concentrations of Al and K, positively correlated (Fig. S4a), indicating K mainly comes from terrigenous material, not seawater. The presence of terrigenous material influences the content of Na, Sr, Fe, and Mn in whole rock samples of the dolostone from the higher terrace, while its influence is weaker in the medium and lower terraces. Scatter plots of Al with Na, Sr, Fe, and Mn in higher terrace dolomite samples (Fig. S4c, e, g, i) show significant positive correlation. To eliminate terrigenous influence, samples with Al/(Ca + Mg) > 0.01 were removed (4 data points within dashed circle). After removal (Fig. S4d, f, h, j), no correlation between Al and Na, Sr, Fe, and Mn is evident, confirming the method's effectiveness. Thus, contaminated data are excluded from dolomitization fluid analysis.

Correlation analysis shows terrigenous material affects REE concentrations in higher terrace whole rock samples, with weaker effects on medium and lower terraces. Scatter plots of Zr, Sc, Th with ΣREEs in higher terrace dolomite samples (Fig. S4k, m, o) show significant positive correlation. Removing samples with Al/(Ca + Mg) > 0.01 (4 data points within dashed circle) eliminates correlation between Zr, Sc, Th, and ΣREE (Fig. S4l, n, p), validating the method. Contaminated data are excluded from dolomitization fluid analysis.

Furthermore, we applied the same method to analyze the trace elements and rare earth elements in dolostone and partially dolomitized limestone samples obtained through LA-ICP-MS. The results showed that the influence of terrigenous material on these data was minimal (Fig. S4q-x).

References

Bau, M., Dulski, P. Distribution of yttrium and rare-earth elements in the Penge and Kuruman iron-formations, Transvaal Supergroup, South Africa. Precambrian Research, 1996, 79(1-2): 37-55.

Kawabe, I., Toriumi, T., Ohta, A., et al. Monoisotopic REE abundances in seawater and the origin of seawater tetrad effect. Geochemical Journal, 1998, 32(4): 213-229.

McLennan, S. M. Rare earth elements in sedimentary rocks; influence of provenance and sedimentary processes. Reviews in Mineralogy and Geochemistry, 1989, 21(1): 169-200.

Supplementary Tables

Table S1. Major, trace elements and *in-situ* laser analysis of the LWMF, Sichuan Basin

Region	Lithology		MgO	CaO	K	Na	Fe	Al	Mn	Sr	Mg/Ca	Mn/Sr	Rb/Sr	Al/(Ca+Mg)	Sc	Zr	Th	REE	Ce/Ce*	Eu/Eu*	(La/Yb)n
			%		ppm										ppm						
Central Sichuan Basin (the higher terrace)	DG (n=13)	min	22.42	29.59	771.48	574.19	909.33	688.04	295.85	51.50	0.63	4.34	0.01	0.0020	0.58	0.06	0.15	4.30	4.51	0.67	2.01
		max	23.01	30.57	3077.94	2463.02	6480.58	3334.33	1339.91	168.12	0.65	9.10	0.12	0.0110	3.66	3.81	6.95	11.95	5.54	1.07	7.71
		av.	22.74	29.91	1511.87	928.88	2941.40	2001.63	584.31	86.68	0.64	6.72	0.05	0.0067	1.35	0.64	1.39	7.51	5.00	0.94	3.46
		SD	0.17	0.28	608.08	601.35	1704.72	817.30	318.56	38.29	0.00	1.48	0.04	0.0029	0.97	1.11	2.07	2.78	0.30	0.11	1.53
	DM (n=6)	min	22.37	29.41	586.13	514.66	1538.87	740.96	319.86	50.24	0.64	5.66	0.02	0.0020	0.60	0.13	0.14	6.58	4.50	0.90	2.35
		max	22.98	30.21	1857.40	2585.57	7728.00	3646.29	1391.89	183.60	0.64	9.98	0.11	0.0130	3.86	3.25	4.22	10.42	5.05	1.00	5.22
		av.	22.73	29.90	1065.16	988.12	3281.54	1851.47	579.88	78.84	0.64	7.40	0.05	0.0063	1.31	0.83	1.31	8.61	4.81	0.96	3.48
		SD	0.22	0.27	472.96	791.70	2290.60	1072.93	402.05	51.99	0.00	1.55	0.04	0.0039	1.26	1.22	1.52	1.40	0.20	0.04	1.12
	CD (n=8)	min	22.36	29.35	371.48	516.56	2028.52	582.18	370.20	46.60	0.63	4.88	0.01	0.0020	0.76	0.14	0.53	4.19	4.36	0.87	1.97
		max	23.06	30.63	2401.26	1576.04	5036.31	2866.08	885.98	146.14	0.64	8.83	0.14	0.0100	3.05	4.87	6.17	11.68	5.70	1.04	7.48
		av.	22.80	30.01	1341.19	732.05	3158.51	1824.25	534.05	80.92	0.64	6.79	0.05	0.0063	1.21	1.02	1.70	7.30	5.03	0.96	3.62
		SD	0.24	0.39	643.26	345.04	1076.05	757.37	165.49	29.33	0.00	1.31	0.04	0.0026	0.76	1.58	1.84	2.44	0.49	0.05	1.83
	In-situ DM (n=19)	min	20.34	29.24	515.87	250.33	1040.56	181.62	273.15	39.42	0.55	4.45	0.01	0.0010	0.05	0.17	0.04	3.14	4.59	0.83	3.74
		max	21.89	31.22	888.01	734.42	2179.49	580.77	387.17	73.30	0.63	8.00	0.03	0.0020	0.16	2.02	0.36	6.71	6.73	1.34	15.48
		av.	21.15	29.90	677.37	432.88	1359.51	415.58	299.94	52.99	0.60	5.83	0.01	0.0015	0.10	0.59	0.11	4.31	5.33	1.03	7.53
		SD	0.49	0.50	115.14	147.02	334.29	109.77	27.44	9.81	0.02	1.08	0.01	0.0005	0.03	0.53	0.09	0.88	0.56	0.13	2.87
Southern Sichuan Basin (the medium terrace)	DG (n=7)	min	19.25	29.16	245.41	507.62	1180.90	732.10	315.17	70.55	0.54	4.00	0.02	0.0030	0.32	0.05	0.12	3.09	4.54	0.82	2.33
		max	20.39	29.94	1087.41	585.27	1767.27	1068.81	325.52	79.30	0.58	4.52	0.07	0.0040	0.94	0.13	0.67	5.62	5.00	1.09	4.68
		av.	19.76	29.59	566.79	542.67	1542.90	820.48	319.81	74.57	0.56	4.30	0.04	0.0031	0.62	0.09	0.32	4.19	4.79	0.95	3.12
		SD	0.40	0.25	329.90	26.07	191.96	121.55	3.66	3.54	0.01	0.22	0.02	0.0004	0.26	0.03	0.19	1.05	0.15	0.11	0.84
	CD (n=10)	min	19.18	28.92	514.25	507.01	1184.55	1289.51	213.07	60.94	0.52	2.93	0.02	0.0050	0.48	0.02	0.24	4.44	3.35	0.70	2.09
		max	19.95	31.16	1983.76	577.85	2333.33	2091.14	416.06	88.93	0.58	5.64	0.09	0.0080	1.22	0.53	0.78	7.95	5.33	1.03	3.09
		av.	19.60	29.77	1242.11	540.70	1824.42	1598.54	318.43	76.47	0.56	4.21	0.06	0.0060	0.88	0.29	0.47	6.16	4.62	0.88	2.53
		SD	0.28	0.67	431.26	22.02	387.54	305.62	60.83	9.11	0.02	0.95	0.02	0.0011	0.23	0.17	0.18	1.18	0.54	0.11	0.32
	DM (n=5)	min	20.02	28.49	1172.83	530.20	1455.94	1342.12	238.15	75.22	0.59	3.02	0.04	0.0050	0.15	0.15	0.07	3.14	4.54	0.82	2.12
		max	20.98	28.95	1443.14	679.36	2337.32	1530.22	339.81	94.26	0.62	4.13	0.07	0.0060	0.93	0.51	0.85	4.92	4.91	1.06	2.88
		av.	20.47	28.82	1264.43	599.57	2012.64	1416.21	299.44	81.76	0.60	3.68	0.05	0.0052	0.46	0.32	0.35	4.14	4.67	0.96	2.49
		SD	0.35	0.20	108.86	60.18	357.71	91.57	39.87	7.92	0.01	0.55	0.01	0.0004	0.30	0.14	0.30	0.69	0.15	0.09	0.28
	In-situ DG (n=5)	min	20.05	29.00	428.22	234.79	1270.94	132.43	174.21	69.09	0.57	2.14	0.00	0.0000	0.03	0.08	0.07	1.90	4.28	0.88	1.06
		max	21.69	29.70	806.29	502.94	1621.39	599.62	259.63	108.16	0.63	3.76	0.02	0.0020	0.25	1.45	0.37	3.32	6.73	1.15	2.46
		av.	20.69	29.47	600.23	388.49	1515.82	378.22	216.32	84.55	0.59	2.62	0.01	0.0012	0.11	0.58	0.25	2.68	5.70	1.02	1.54
		SD	0.79	0.29	154.02	97.01	140.84	194.97	32.77	14.37	0.03	0.67	0.01	0.0008	0.08	0.57	0.12	0.51	1.23	0.11	0.56
	In-situ CC (n=4)	min	0.40	52.58	385.22	15.99	610.20	221.23	87.14	72.66	0.01	0.97	0.00	0.0010	0.04	0.05	0.06	3.20	2.77	0.70	0.98
		max	1.84	54.60	629.11	164.87	876.69	500.81	176.54	108.65	0.03	1.62	0.01	0.0020	0.24	0.69	0.35	4.37	6.24	1.17	2.12
		av.	1.03	53.80	490.41	90.12	785.89	378.24	118.03	96.86	0.02	1.21	0.00	0.0015	0.13	0.50	0.21	3.76	4.76	0.98	1.47
		SD	0.65	0.97	109.17	85.46	119.73	116.48	39.87	16.44	0.01	0.29	0.01	0.0006	0.08	0.30	0.12	0.48	1.63	0.20	0.48
Eastern Sichuan Basin (the lower terrace)	DG (n=8)	min	21.18	29.29	321.45	432.17	627.44	317.56	84.21	58.62	0.58	0.88	0.00	0.0010	0.06	0.02	0.04	2.56	4.60	0.89	2.13
		max	21.89	30.71	1335.52	567.03	1766.04	1816.28	191.16	104.60	0.63	2.09	0.08	0.0060	1.34	0.41	0.78	6.09	5.01	1.06	4.01
		av.	21.65	29.91	736.83	509.50	1310.95	658.06	129.12	87.36	0.61	1.50	0.04	0.0023	0.50	0.13	0.25	4.49	4.77	0.97	3.01
		SD	0.23	0.53	295.21	50.09	461.14	515.39	33.92	13.56	0.02	0.40	0.03	0.0017	0.44	0.12	0.27	1.09	0.18	0.06	0.60
	DM (n=6)	min	21.14	29.47	648.23	501.52	627.44	1080.68	83.24	80.97	0.59	1.02	0.02	0.0040	0.25	0.05	0.23	4.66	4.49	0.84	1.89
		max	21.82	30.44	1389.34	585.23	1603.93	1581.16	196.09	95.27	0.62	2.38	0.04	0.0050	0.56	0.22	0.56	5.26	5.01	1.03	4.12
		av.	21.45	30.03	1059.40	540.28	1185.52	1265.16	121.22	85.31	0.60	1.43	0.03	0.0043	0.40	0.12	0.36	4.84	4.78	0.94	3.14
		SD	0.27	0.36	298.26	31.99	327.17	214.33	44.28	5.19	0.01	0.55	0.01	0.0005	0.12	0.06	0.11	0.22	0.24	0.08	0.79
	CD (n=4)	min	21.61	29.12	303.95	424.51	891.71	568.14	86.00	80.00	0.63	0.93	0.01	0.0020	0.46	0.04	0.06	3.16	4.41	0.90	2.47
		max	21.88	29.27	900.81	498.78	1256.26	845.17	319.00	98.56	0.63	3.58	0.06	0.0030	0.87	0.16	0.90	4.86	4.61	1.07	3.20
		av.	21.80	29.19	582.82	461.74	1019.10	757.75	221.50	90.85	0.63	2.49	0.03	0.0028	0.61	0.10	0.44	3.77	4.49	0.95	2.83
		SD	0.13	0.06	301.04	30.32	163.02	128.97	104.45	7.80	0.00	1.27	0.02	0.0005	0.18	0.05	0.36	0.75	0.08	0.08	0.34
	MS (n=7)	min	1.05	49.98	384.08	179.46	419.69	211.70	108.43	134.10	0.02	0.46	0.01	0.0010	0.16	0.04	0.12	2.57	3.50	0.95	2.49
		max	3.70	53.59	991.02	209.92	1068.17	846.81	154.90	237.64	0.06	0.99	0.04	0.0030	0.44	0.26	0.29	4.84	5.59	1.09	4.26
		av.	1.76	51.29	664.88	193.60	744.88	514.14	128.12	187.77	0.03	0.71	0.02	0.0019	0.27	0.14	0.24	3.80	4.93	1.03	3.42
		SD	0.98	1.25	246.69	9.69	218.40	245.81	18.01	36.52	0.02	0.16	0.01	0.0009	0.11	0.08	0.06	0.76	0.69	0.05	0.56
	In-situ DG (n=5)	min	19.71	29.63	220.07	224.93	459.41	79.66	82.35	43.23	0.56	0.66	0.00	0.0000	0.03	0.11	0.06	2.18	4.10	0.69	0.87
		max	21.01	30.05	530.01	377.81	689.90	469.45	103.68	124.03	0.60	1.91	0.07	0.0020	0.15	1.88	0.49	3.12	6.08	1.28	4.26
		av.	20.45	29.79	342.15	331.28	610.08	206.25	89.61	74.85	0.58	1.33	0.04	0.0010	0.06	1.06	0.22	2.70	4.86	0.99	2.55
		SD	0.48	0.17	115.29	62.54	90.00	151.30	8.69	29.73	0.02	0.45	0.03	0.0007	0.05	0.71	0.20	0.34	0.80	0.26	1.29
	In-situ CC (n=11)	min	0.16	47.88	198.93	9.64	134.17	100.25	31.79	100.71	0.00	0.24	0.00	0.0000	0.00	0.01	0.00	1.92	3.98	0.54	1.81
		max	4.44	55.66	499.16	200.57	470.72	696.35	69.64	136.48	0.08	0.65	0.02	0.0030	0.29	1.24	0.49	4.36	5.63	1.16	12.92
		av.	0.78	53.97	302.67	99.69	268.40	252.56	41.06	119.23	0.01	0.35	0.00	0.0010	0.11	0.33	0.21	2.92	4.74	0.89	6.36
		SD	1.22	2.34	89.27	60.80	116.69	161.23	12.01	13.10	0.02	0.13	0.01	0.0008	0.09	0.36	0.18	0.76	0.61	0.19	3.35
	Partially dolomitized limestone (n=8)	min	/	/	/	/	/	/	/	83.32	0.14	0.62	/	/	/	/	/	/	/	/	/
		max	/	/	/	/	/	/	/	176.00	0.25	1.81	/	/	/	/	/	/	/	/	/
		av.	/	/	/	/	/	/	/	125.85	0.18	1.17	/	/	/	/	/	/	/	/	/
		SD	/	/	/	/	/	/	/	34.57	0.04	0.44	/	/	/	/	/	/	/	/	/

Table S2. The crystalline order of dolomite for the LWMF, Sichuan Basin

Region	Lithology		Order degree	Region	Lithology		Order degree	Region	Lithology		Order degree
Central Sichuan Basin (the higher terrace)	DG (n=9)	min	0.66	Southern Sichuan Basin (the medium terrace)	DG (n=5)	min	0.55	Eastern Sichuan Basin (the lower terrace)	DG (n=5)	min	0.50
		max	0.83			max	0.74			max	0.75
		av.	0.73			av.	0.65			av.	0.65
		SD	0.06			SD	0.07			SD	0.10
	DM (n=3)	min	0.61		CD (n=3)	min	0.67		DM (n=5)	min	0.56
		max	0.65			max	0.71			max	0.75
		av.	0.63			av.	0.69			av.	0.63
		SD	0.02			SD	0.02			SD	0.08
	CD (n=3)	min	0.63		DM (n=2)	min	0.62		CD (n=3)	min	0.67
		max	0.81			max	0.64			max	0.70
		av.	0.74			av.	0.63			av.	0.69
		SD	0.10			SD	0.01			SD	0.02

Table S3. Carbon, oxygen and strontium isotope data for the LWMF, Sichuan Basin

Region	Lithology		δ^{13}C	δ^{18}O	^{87}Sr/^{86}Sr	Region	Lithology		δ^{13}C	δ^{18}O	^{87}Sr/^{86}Sr
			VPDB						VPDB		
Central Sichuan Basin (the higher terrace)	DG (n=13)	min	-1.17	-7.71	0.709185	Southern Sichuan Basin (the medium terrace)	*In-situ* CC (n=4)	min	-0.13	-8.87	0.708821
		max	-0.07	-5.61	0.713990			max	0.36	-8.47	0.709142
		av.	-0.63	-6.72	0.710769			av.	0.11	-8.75	0.708963
		SD	0.35	0.58	0.001530			SD	0.22	0.19	0.000135
	DM (n=6)	min	-0.64	-6.80	0.709427	Eastern Sichuan Basin (the lower terrace)	DG (n=8)	min	-0.37	-9.27	0.709070
		max	0.00	-5.36	0.712899			max	0.29	-7.02	0.710249
		av.	-0.28	-6.03	0.710118			av.	-0.27	-8.02	0.709781
		SD	0.29	0.51	0.001368			SD	0.23	0.72	0.000443
	CD (n=8)	min	-0.84	-7.32	0.709371		DM (n=6)	min	-0.65	-6.87	0.708851
		max	0.00	-5.92	0.714694			max	0.91	-5.26	0.709962
		av.	-0.33	-6.70	0.711019			av.	0.17	-5.86	0.709571
		SD	0.27	0.52	0.001642			SD	0.58	0.57	0.000440
	In-situ DM (n=9)	min	-0.37	-6.96	0.710211		CD (n=4)	min	-0.58	-7.20	0.709144
		max	0.23	-5.50	0.710686			max	-0.23	-7.01	0.709854
		av.	-0.13	-6.32	0.710429			av.	-0.40	-7.14	0.709384
		SD	0.23	0.50	0.000138			SD	0.15	0.09	0.000319
Southern Sichuan Basin (the medium terrace)	DG (n=7)	min	-0.41	-9.02	0.709255		MS (n=7)	min	-0.78	-8.95	0.708693
		max	0.66	-7.07	0.709928			max	0.31	-7.91	0.709135
		av.	0.16	-7.84	0.709696			av.	-0.41	-8.46	0.708880
		SD	0.47	0.80	0.000253			SD	0.39	0.36	0.000155
	CD (n=10)	min	-1.90	-8.38	0.709546		*In-situ* DG (n=4)	min	-0.57	-6.71	0.709372
		max	-0.28	-7.18	0.709961			max	0.65	-5.90	0.709883
		av.	-1.20	-7.79	0.709790			av.	-0.03	-6.34	0.709578
		SD	0.57	0.39	0.000137			SD	0.51	0.39	0.000251
	DM (n=5)	min	-2.52	-8.58	0.709732		*In-situ* CC (n=5)	min	-0.86	-8.81	0.708758
		max	-0.01	-7.23	0.709988			max	-0.08	-8.27	0.709084
		av.	-1.85	-7.72	0.709854			av.	-0.44	-8.47	0.708954
		SD	1.05	0.55	0.000101			SD	0.28	0.22	0.000141
	In-situ DG (n=4)	min	-1.03	-7.80	0.709558		Partially dolomitized limestone (n=8)	min	-0.62	-8.03	/
		max	-0.51	-7.03	0.709911			max	1.08	-5.69	/
		av.	-0.72	-7.41	0.709726			av.	0.40	-7.22	/
		SD	0.22	0.39	0.000148			SD	0.54	0.75	/

Table S4. Calcium isotope data for the LWMF, Sichuan Basin

Region	Lithology		δ$^{44/40}$Ca	Region	Lithology		δ$^{44/40}$Ca
			(‰, Seawater)				(‰, Seawater)
Central Sichuan Basin (the higher terrace)	DG (n=4)	min	-1.27	Southern Sichuan Basin (the medium terrace)	DM (n=2)	min	-1.07
		max	-0.94			max	-0.94
		av.	-1.14			av.	-1.01
		SD	0.14			SD	0.09
	DM (n=1)	min	-1.05	Eastern Sichuan Basin (the lower terrace)	DG (n=2)	min	-1.49
		max	-1.05			max	-1.44
		av.	-1.05			av.	-1.47
		SD	/			SD	0.04
	CD (n=2)	min	-1.18		DM (n=6)	min	-1.47
		max	-1.17			max	-1.23
		av.	-1.18			av.	-1.35
		SD	0.01			SD	0.08
Southern Sichuan Basin (the medium terrace)	DG (n=3)	min	-1.27		MS (n=4)	min	-1.11
		max	-1.18			max	-1.01
		av.	-1.23			av.	-1.07
		SD	0.05			SD	0.05
	CD (n=2)	min	-1.25		Partially dolomitized limestone (n=8)	min	-1.17
		max	-1.06			max	-0.94
		av.	-1.16			av.	-1.08
		SD	0.13			SD	0.08

Supplementary figures

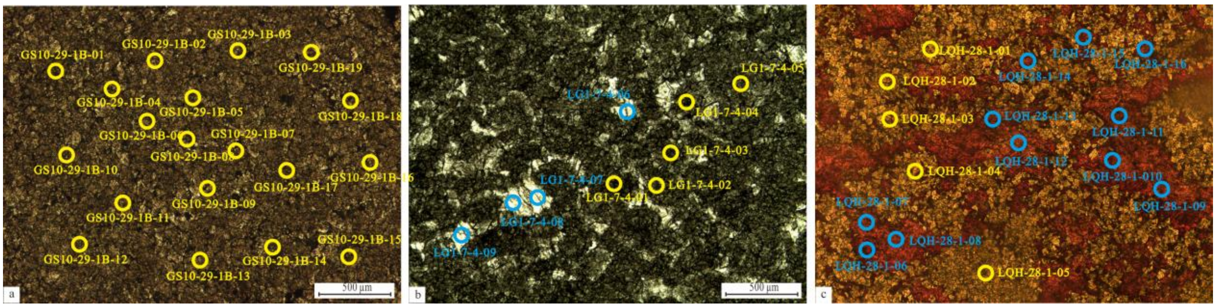

Fig. S1. (a) Dolomudstone, GS10, 4630.8m, PPL; (b) Calcareous dolograinstone, LG1, 4835.08m, PPL; (c) Calcareous dolograinstone, Laoqihe outcrop, PPL;

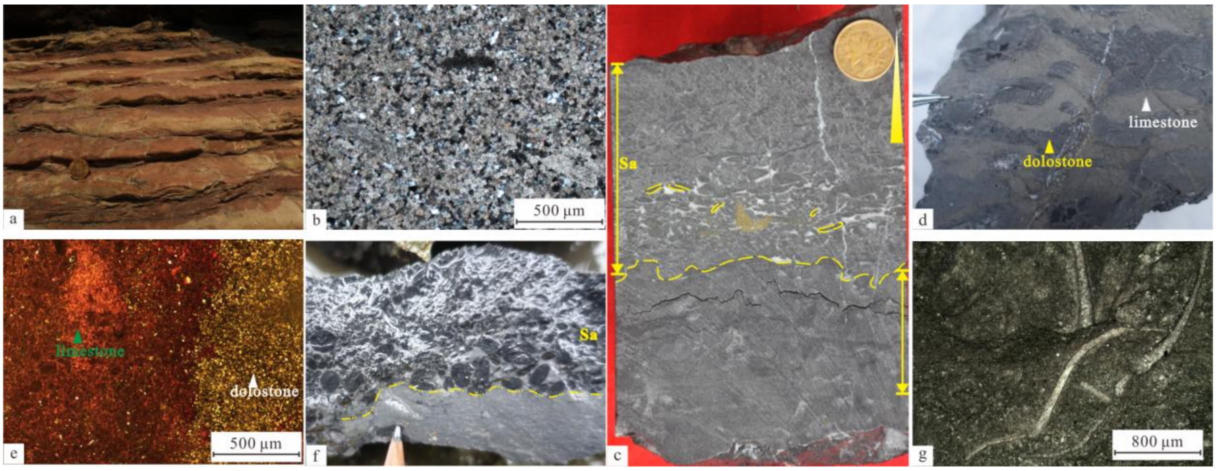

Fig. S2. Depositional setting of the Longwangmiao Formation in the Sichuan Basin. (a) Vermilion sandy mudstone, mixed tidal flat, Fandian outcrop, Southern Sichuan Basin (the medium terrace); (b) sandy dolostones, with terrigenous clasts, CPL, mixed tidal flat, MX202, 4750.84 m, Central Sichuan Basin (the higher terrace); (c) tempestite beds, Sa: Graded bedding section. Gravel dolostones and fine dolograinstones with graded or massive beds; yellow dotted line: irregular scour surfaces and groove casts were developed on the bottom and had abrupt contact with the underlying layers, GS10, 4689.39 ~ 4689.56 m, Central Sichuan Basin (the higher terrace); (d) patchy dolostone, black mottles and white mottles are irregular and staggered in size, Laoqihe outcrop, Eastern Sichuan Basin (the lower terrace); (e) calcareous dolostone, PPL, calcite with red color under staining of Alizarin Red solution, Laoqihe outcrop, Eastern Sichuan Basin (the lower terrace); (f) tempestite beds, grainstones, gravel limestones and fine grainstones with graded or massive beds; yellow dotted line: irregular scour surfaces and groove casts were developed on the bottom and had abrupt contact with the underlying layers, Shiliu outcrop, Eastern Sichuan Basin (the lower terrace) and (g) bioclastic limestone, high shale content, PPL, Shiliu outcrop, Eastern Sichuan Basin (the lower terrace).

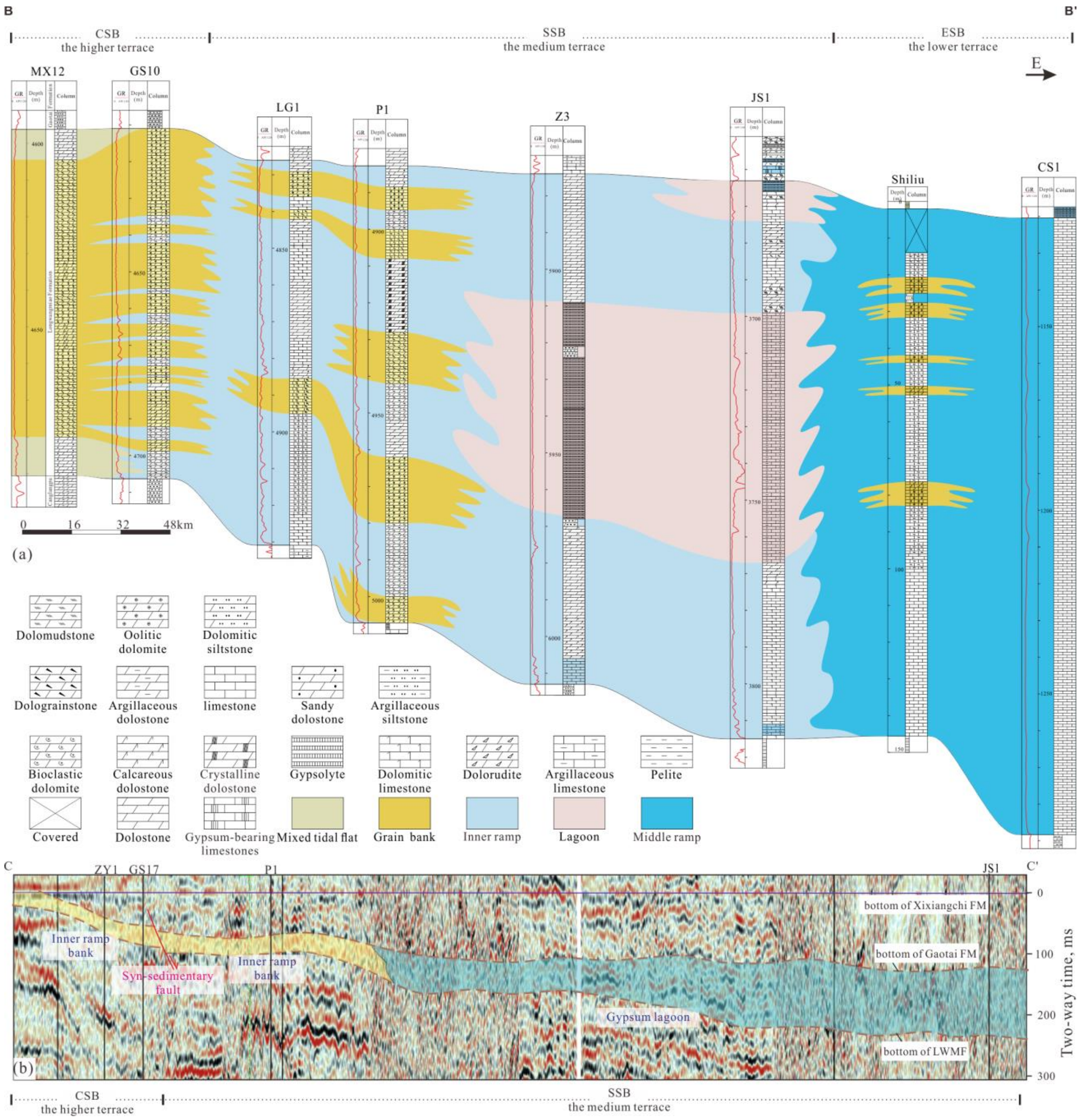

Fig. S3. (a) Lateral correlation profile of the Longwangmiao Formation Facies from the borehole MX12 to borehole CS1, Sichuan Basin (the location of the profile can be found in Fig. 1 as marked by B-B') and (b) seismic reflection characteristics of the paleogeography of the Longwangmiao Formation, with the bottom of the Xixiangchi Formation horizon flattening through the boreholes ZY1 and JS1(the location of the profile can be found in Fig. 1 as marked by C-C').

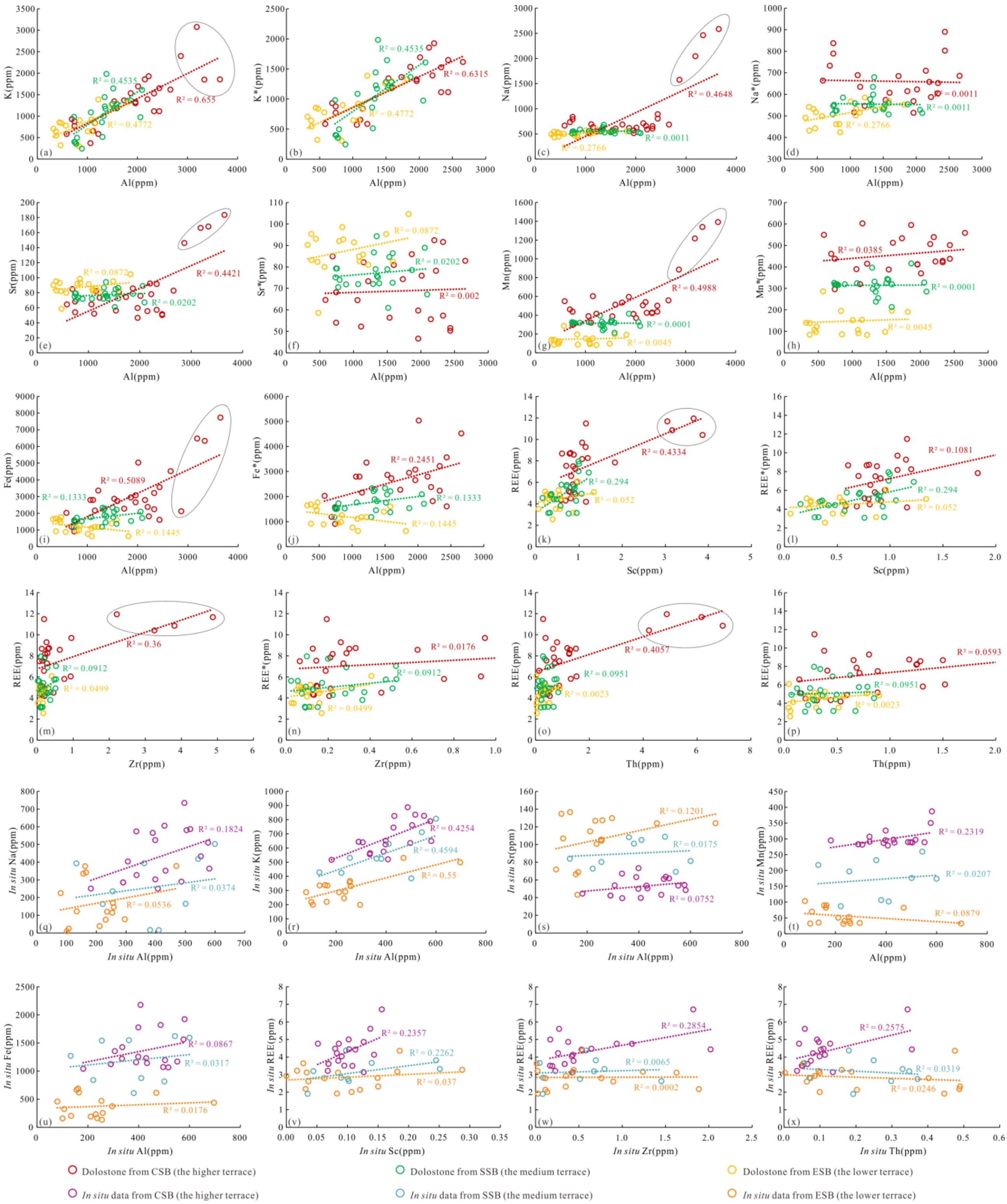

Fig. S4. Scatterplots of the trace elements within the dolostones in Central Sichuan Basin (the higher terrace), Southern Sichuan Basin (the medium terrace) and Eastern Sichuan Basin (the lower terrace). Scatterplot of (a) K-Al; (b) K*-Al; (c) Na-Al; (d) Na*-Al; (e) Sr-Al; (f) Sr*-Al; (g) Mn-Al; (h) Mn*-Al; (i) Fe-Al; (j) Fe*-Al; (k) REE-Sc; (l) REE*-Sc; (m) REE-Zr; (n) REE*-Zr; (o) REE-Th; (p) REE*-Th; (q) *in-situ* Na- *in-situ* Al; (r) *in-situ* K- *in-situ* Al; (s) *in-situ* Sr- *in-situ* Al; (t) *in-situ* Mn- *in-situ* Al; (u) *in-situ* Fe- *in-situ* Al; (v) *in-situ* REE- *in-situ* Sc; (w) *in-situ* REE- *in-situ* Zr; (x) *in-situ* REE- *in-situ* Th.